

RESEARCH ARTICLE

Open Access



Evaluation of serum tRF-23-Q99P9P9NDD as a potential biomarker for the clinical diagnosis of gastric cancer

Yu Zhang^{1,2,3†}, Xinliang Gu^{1,2,3†}, Xinyue Qin^{1,2,3}, Yuejiao Huang^{1,4*} and Shaoqing Ju^{2*} 

Abstract

Background: Gastric cancer (GC) is one of the diseases that endanger human health with high morbidity and mortality. The positive rates of traditional biomarkers in the diagnosis of GC are low, so it is necessary to find biomarkers with high sensitivity to increase the detection rate. tRNA-derived small RNAs (tsRNAs) are novel small non-coding RNAs with specific biological functions and aberrant expression in cancer. In this study, we focused on the potential of tRNA-derived small RNAs as GC biomarkers.

Methods: The differentially expressed tsRNAs in three pairs of GC tissues were screened with high-throughput sequencing and verified using the TCGA database and Quantitative real-time PCR. The methodological evaluation of tRF-23-Q99P9P9NDD was verified by agarose gel electrophoresis, RIN evaluation, and Sanger sequencing. The Chi-square test was used to evaluate the relationship between the tRF-23-Q99P9P9NDD expression and clinicopathological parameters. Kaplan–Meier survival analysis was used to evaluate the effect of the tRF-23-Q99P9P9NDD expression on survival. Additionally, the receiver operating characteristic curve (ROC) was used to evaluate the diagnostic efficacy of tRF-23-Q99P9P9NDD in GC.

Results: Differential expression of serum tRF-23-Q99P9P9NDD could distinguish GC patients from gastritis patients and healthy donors. Chi-square test showed that high expression of tRF-23-Q99P9P9NDD was significantly associated with T stage, lymph node metastasis, TNM stage, and nerve/vascular invasion. Kaplan–Meier curve showed that patients with high expression of tRF-23-Q99P9P9NDD had a lower survival rate than patients with low expression of this biomarker. ROC analysis showed that, compared with conventional biomarkers, the efficacy of tRF-23-Q99P9P9NDD was higher, which was improved by the combination of biomarkers, and even in the early stages. Finally, we preliminarily predicted the downstream of tRF-23-Q99P9P9NDD in GC cells.

Conclusions: The expression of tRF-23-Q99P9P9NDD in GC serum can identify GC patients, and it has higher efficacy than conventional biomarkers even in the early stages. Furthermore, tRF-23-Q99P9P9NDD can monitor the postoperative conditions of GC patients.

Keywords: tRNA-derived small RNAs, tRF-23-Q99P9P9NDD, Gastric cancer, Biomarker, Diagnosis

[†]Yu Zhang and Xinliang Gu should be considered joint first author

*Correspondence: huangyuejiao20@126.com; jsq814@hotmail.com

² Department of Laboratory Medicine, Affiliated Hospital of Nantong University, Xisi Road, No. 20, Nantong, China

⁴ Department of Medical Oncology, Affiliated Hospital of Nantong University, Xisi Road, No. 20, Nantong, China

Full list of author information is available at the end of the article

Introduction

Gastric cancer (GC) is a common digestive tract malignancy worldwide. The incidence of GC has gradually decreased with increasing research on the eradication of *Helicobacter pylori* infection and changes in dietary structure (Piazuelo and Correa 2013; Wu et al. 2019). Nonetheless, GC remains one of the top three cancers in



China (Wang et al. 2019). Most cases of GC are adenocarcinomas, with intestinal adenocarcinomas being more common, and most are located in the gastric antrum and body (den Hoed and Kuipers 2016). The high mortality rate of GC is mainly due to late diagnosis or metastasis of the tumor (Dassen et al. 2010), which results in patients missing the best treatment period and usually having a poor prognosis. The gold standard for GC diagnosis is upper gastrointestinal endoscopy, but this minimally invasive procedure tends to cause patient discomfort. The technique is influenced by the skills of the endoscopist, making diagnostic results relatively variable (Park et al. 2014). Therefore, non-invasive cancer biomarkers released from tumor tissue into the body fluids have attracted attention (Kalniņa et al. 2015; Wang et al. 2020). Current GC biomarkers, including carcinoembryonic antigen (CEA), carbohydrate antigen 199 (CA199), and carbohydrate antigen 724 (CA724), have low positive rates in GC diagnosis (Shimada et al. 2014). Therefore, finding new tumor biomarkers with high sensitivity and specificity is necessary to screen and diagnose GC patients.

A non-coding RNA (ncRNA) is an RNA that does not code for proteins. This class of RNAs has been a hot topic of research and has been shown to play an important role in cancer (Li et al. 2014). It includes long non-coding RNAs (lncRNAs), circular RNAs (circRNAs), pseudogenes, Piwi-interacting RNAs (piRNAs), and microRNAs (miRNAs). Xu et al. identified circRNA_0001178 and circRNA_0000826 as biomarkers of liver metastasis in human colorectal cancer (Xu et al. 2019). According to Chao et al. lncRNA-D16366 could be a promising biomarker for the diagnosis and prognosis of hepatocellular carcinoma (Chao and Zhou 2019). However, these diagnostic biomarkers have certain limitations. Therefore, a search for new biomarkers to assist clinical diagnosis has begun. tRNA-derived small RNAs (tsRNAs) are a new type of non-coding short RNAs that have been gaining popularity. Because tsRNAs have a high abundance and good stability in body fluids, they can become tumor biomarkers (Gu et al. 2021). The biological functions of tsRNAs have been demonstrated to influence tumor cell proliferation, migration, and metastasis (Yu et al. 2020).

tsRNAs, which include tRNA-derived fragments (tRFs) and tRNA halves (tiRNAs), are formed by specialized cleavage of mature tRNAs or pre-tRNAs (Zhu et al. 2019a, b). tRFs, which are 14–30 nucleotides (nt) long and resemble miRNAs with 5'-phosphate and 3'-hydroxyl groups, are attracting increasing interest. tRFs can be divided into five main subclasses, namely, i-tRF, tRF-1, tRF-2, tRF-3, and tRF-5, according to the different digestive sites of Angiogenin (ANG), Dicer, or other RNA enzymes. tiRNAs are usually about 31–40

nt long. Under stressful situations, such as phosphate deprivation, amino acid deficiency, hypoxia, oxidative stress, and viral infection, tiRNAs are generated by the cleavage of anticodon loops of mature tRNAs. 5'tiRNA and 3'tiRNA are the two kinds of tiRNAs (Xie et al. 2020; Zong et al. 2021).

tsRNAs can affect gene expression at both the transcriptional and post-transcriptional stages, with RNA silencing, translation regulation, and epigenetic regulation as the underlying molecular processes (Xie et al. 2020). For example, tRF-3019a forms an RNA-induced silencing complex (RISC) with Ago2 protein, which is directly bound to the 3'UTR of FBXO47 mRNA and degrades mRNA to inhibit translation (Zhang et al. 2020). Under stress, pseudouridylation synthase 7 (PUS7) could bind to tsRNAs and generated mTOG-Ψ8, which is preferentially bound to PABPC1, replacing the translation initiator eIF4G/eIF4E, thus inhibiting the translation (Guzzi et al. 2018). In addition, some tsRNAs could influence the offspring metabolism by regulating epigenetics (Chen et al. 2016). Thus, tsRNAs affect the progress of cancer through these specific molecular mechanisms. For example, Tong et al. demonstrated that tRF-3017A could accelerate GC progression by targeting NELL2 in a manner that resembles miRNA-mediated mRNA silencing (Tong et al. 2020). 5'-tiRNA^{Val}, according to Mo et al. targeted FZD3 and thereby suppressed the Wnt/β-Catenin signaling pathway in breast cancer (Mo et al. 2019). In addition, in breast cancer, plasma tRF-Arg-CCT-017, tiRNA-Phe-GAA-003, and tRF-Gly-CCC-001 could be used as novel diagnostic markers and the first two molecules had high prognostic value (Wang et al. 2021). Moreover, tsRNAs may also serve as therapeutic targets for diseases (Sun et al. 2018; Yu et al. 2021), indicating that tsRNAs have increased research value in cancer. Therefore, our team focused on the relationship between the dysregulation of tsRNAs and GC.

High-throughput sequencing technology was used in this study to test for differentially expressed tsRNAs in GC tissues, among which the highly expressed tRF-23-Q99P9P9NDD was selected for further research. We found for the first time that tRF-23-Q99P9P9NDD expression in GC serum was notably higher than normal, and it can be an excellent prognostic biomarker to monitor tumor progression. Furthermore, receiver operating characteristic curve (ROC) analysis revealed that tRF-23-Q99P9P9NDD had higher diagnostic efficacy than CEA, CA199, and CA724, and the diagnostic efficacy was further improved when combined. Therefore, we believe that tRF-23-Q99P9P9NDD has the potential to become a novel biomarker for the diagnosis and prognostic monitoring of GC.

Materials and methods

Clinical serum and tissue samples

All of the samples in this study were collected between September 2016 and October 2020, following the ethical guidelines of the World Medical Association. The samples included serum samples from 124 preoperative GC patients, 50 gastritis patients, 119 healthy donors, and 40 postoperative GC patients taken from the Clinical Laboratory of Affiliated Hospital of Nantong University. In addition, 50 pairs of GC tissues and their matched paracancer tissues collected in the Department of Pathology of our hospital were immediately frozen in liquid nitrogen before being moved to -80°C refrigerators for long-term preservation. All of the above patients had their diagnoses confirmed by pathology, did not undergo neoadjuvant radiation, chemotherapy, or targeted therapy, and signed informed consent according to ethical guidelines. The Ethics Committee of Affiliated Hospital of Nantong University has approved this project (ethical review report number: 2018-L055).

High-throughput sequencing

Trizol was used to isolate total RNA, and RNA quantity and integrity were assessed using Qubit[®]2.0 and Agilent 2200 TapeStation, respectively. According to the instructions of the manufacturer, 1 μg total RNA of each sample was prepared by NEBNext[®] Multiplex Small RNA Library Prep Set for Illumina to prepare a small RNA library. The library was sequenced using a HiSeq 2500 SE50 sequencing system. The clean reads measured were compared with MINTbase using MINTmap software, and new tsRNA prediction was performed for reads not included in MINTbase. EdgeR was used to analyze tsRNAs changes across groups.

Cell culture

Chinese Academy of Sciences (Shanghai, China) provided human GC cell lines (HGC-27, AGS, MKN-45, SGC-7901, BGC-823) and human gastric mucosal epithelial cell lines (GES-1). All cells were cultured in RPMI 1640 medium (Corning, Manassas, VA, USA) containing 10% fetal bovine serum (Gibco, Waltham, MA, USA), supplemented with 1% penicillin and streptomycin (HyClone, Logan, UT, USA). The culture environment is 37°C and 5% CO_2 humidification incubator.

Total RNA extraction and cDNA synthesis

A total RNA purification kit and a rotating column separation kit (BioTeke, Wuxi, Jiangsu, China) were used to extract total RNA from the serum of GC patients, and total RNA in tissue and cell samples was extracted using TRIzol Reagent (Invitrogen, Carlsbad, CA, USA). Specific primers (Ribobio, Guangzhou, Guangdong, China) and a

Revert Aid RT reverse transcription kit (Thermo Fisher Scientific, Waltham, MA, USA) were used to reverse transcribe total RNA into cDNA in a total of 10 μL incubated for 60 min at 42°C , which was then inactivated for 5 min at 70°C . Quantification was required before reaction.

Quantitative real-time PCR (qRT-PCR)

The qRT-PCR reaction in a total volume of 20 μL was performed on QuantStudio 5 (Thermo Fisher Scientific, Waltham, MA, USA), including 10 μL of ChamQ Universal SYBR qPCR Master Mix (Vazyme Biotech Co., Ltd., Nanjing, Jiangsu, China), 5 μL of cDNA, 1 μL of primers, and 3 μL of enzyme-free water. The primers included forward and reversed primers of tRF-23-Q99P9P9NDD and RNU6B (U6). To standardize the relative expression of tRF-23-Q99P9P9NDD, U6 was used as an internal control. All of the primers were synthesized by RiboBio (Ribobio, Guangzhou, Guangdong, China). Upon the reaction, the data was analyzed using the $2^{-\Delta\Delta\text{Ct}}$ method, with the following formula: $\Delta\Delta\text{Ct} = \Delta\text{Ct}_{\text{tumor}[\text{Ct}(\text{target}) - \text{Ct}(\text{reference})]} - \Delta\text{Ct}_{\text{control}[\text{Ct}(\text{target}) - \text{Ct}(\text{reference})]}$.

Nuclear and cytoplasmic RNA isolation assay

Trypsin was used to digest the cultivated MKN-45, HGC-27, and GES-1 cells, and at least 5×10^6 cells were collected into 1.5-mL EP tubes. According to the PARIS[™] kit (Thermo Fisher Scientific, Waltham, MA, USA) procedures and instructions of the reagent manufacturer, 60 μL nuclear and cytoplasmic RNA was extracted and then stored in a -80°C refrigerator.

Room temperature and repeated freezing and thawing experiments

Twenty serum samples were randomly mixed and placed at room temperature (25°C) for 0, 6, 12, 18, and 24 h to extract RNA and detect the expression of tRF-23-Q99P9P9NDD. Subsequently, the mixed serum was freeze-thawed at -80°C and room temperature for 0, 1, 3, 5, and 10 times. RNA was extracted and the expression of tRF-23-Q99P9P9NDD was detected.

Statistical analysis

All of the data in this study were analyzed using SPSS Statistics Version 20.0 (IBM SPSS Statistics, Chicago, IL, USA) and GraphPad Prism 8.0 (GraphPad Software, San Jose, California, USA). The relative expression of tRF-23-Q99P9P9NDD in every group was reported as mean \pm Standard Deviation (SD). The corresponding data in this study were first tested for normality using Normality and Lognormality Tests in GraphPad Prism 8.0, and it was found that all of the data did not conform to the normal distribution. Thus, the Mann–Whitney

U test was used for comparison of two independent groups, the Wilcoxon matched-pairs signed-rank test was used to analyze the expression levels of tRF-23-Q99P9P9NDD in preoperative and postoperative serum of GC patients, as well as GC tissues and their matched para-cancer tissues, and the Kruskal–Wallis H test was used to compare multiple independent groups. The Chi-square test was used to examine the correlation between tRF-23-Q99P9P9NDD and pathological parameters, and Pearson correlation analysis was used to study other correlations in this work. The Kaplan–Meier curve and the log-rank test were used to assess the survival data. The ROC and Area Under Curve (AUC) were created and computed to assess the diagnostic effect of serum tRF-23-Q99P9P9NDD of GC. The Youden index was used to determine the cut-off value of tRF-23-Q99P9P9NDD, and the cut-off values of CEA, CA199, and CA724 were set according to the reference range of the Affiliated Hospital of Nantong University, which was 5 ng/mL, 37 U/mL, and 10 U/mL, respectively. All of the trials were carried out at least three times independently. When the P-value was <0.05, the difference was judged to be statistically significant.

Results

Expression profiles of tsRNAs in GC and screening of tRF-23-Q99P9P9NDD

To obtain differentially expressed tsRNAs in GC tissues, we performed high-throughput sequencing on three GC tissues and their matched para-cancer tissues. According to the sequencing results of tsRNAs, we screened six up-regulated (\log_2 fold change > 1, $P < 0.05$) and six down-regulated (\log_2 fold change < -1, $P < 0.05$) tsRNAs in tumor tissues between the two groups (Fig. 1A). We performed qRT-PCR on these six highly expressed tsRNAs in 10 pairs of GC tissues, and because the expression level of tRF-23-Q99P9P9NDD was most significantly different (Fig. 1B), it was selected for an in-depth study. We validated tRF-23-Q99P9P9NDD in the TCGA stomach adenocarcinoma database, and we found that the expression of tRF-23-Q99P9P9NDD was significantly higher in GC (Fig. 1C), which is consistent with the sequencing results. In addition, we found that the expression levels of tRF-23-Q99P9P9NDD in GC tissues were significantly higher than in para-cancer tissues through qRT-PCR detection ($P = 0.0002$) (Fig. 1D).

tRF-23-Q99P9P9NDD is a sort of tRFs

According to the human genome build (GRCh37/hg19) from the UCSC Genome Browser database (<http://genome-asia.ucsc.edu/biomarker.html>), tRF-23-Q99P9P9NDD is located on chromosome 6P22.1 with coordinates of 27,248,099–27,248,121 (Additional file 1:

Fig. S1A). By checking the basic information of tRF-23-Q99P9P9NDD in MINTbase v2.0 (<https://cm.jefferson.edu/MINTbase/>) and the OncotRF database (<http://bioinformatics.zju.edu.cn/OncotRF/>), we identified tRF-23-Q99P9P9NDD as a 5' tRF (GCTTCTGTAGTGTAG TGGTTATC) of 23 nt in length that was derived from mature tRNA-VAL-CAC, which can be cleaved from tRNA-VAL-CAC-2-1, with the cleavage site located on the D-loop (Additional file 1: Fig. S1B, C). In addition, we found that tRF-23-Q99P9P9NDD had smooth amplification curves and single-peak melting curves (Additional file 1: Fig. S1D, E).

Methodological evaluation of tRF-23-Q99P9P9NDD

To investigate whether the method for detecting the expression level of tRF-23-Q99P9P9NDD can be applied in clinical analysis, we performed a comprehensive evaluation. First, we used a mixture of serum to test its accuracy, and we found that tRF-23-Q99P9P9NDD showed a good inter-assay coefficient of variation (CV) and intra-assay CV, which were 2.29% and 1.53%, respectively (Table 1). Then, the mixed serum samples were divided into two groups, which were placed at room temperature for 0, 6, 12, 18, and 24 h, and repeatedly freeze-thawed for 0, 1, 3, 5, and 10 times. The results of the two groups showed that there was no significant difference in tRF-23-Q99P9P9NDD expression with the changes in these conditions ($P > 0.05$) (Fig. 2A, B), indicating that the detection method of tRF-23-Q99P9P9NDD is not easily affected and has good stability and repeatability. As shown in Fig. 2C, agarose gel electrophoresis (AGE) showed clear bands and RIN evaluation found that the RNA sample had RIN = 9.2, 28S/18S = 1.6, indicating that the RNA sample had good integrity (Fig. 2D). The qRT-PCR product was also detected by AGE, and Fig. 2E shows a single electrophoretic band of about 80 bp and verifies the accuracy of the product. In addition, Sanger sequencing of the product confirmed that it contained the entire tRF-23-Q99P9P9NDD sequence, which was consistent with the sequence of MINTbase v2.0 (Fig. 2F).

Clinical value and prognostic role of tRF-23-Q99P9P9NDD in GC serum

We gathered serum samples from 124 GC patients, 50 gastritis patients, and 119 healthy donors to investigate the diagnostic efficacy of tRF-23-Q99P9P9NDD in the serum of GC patients. The expression level of tRF-23-Q99P9P9NDD in GC patients was substantially higher than that of healthy donors ($P < 0.0001$) and gastritis patients ($P = 0.0009$), but the expression level of tRF-23-Q99P9P9NDD in gastritis patients and healthy donors showed no significant difference ($P = 0.0656$; Fig. 3A). According to the median expression level of

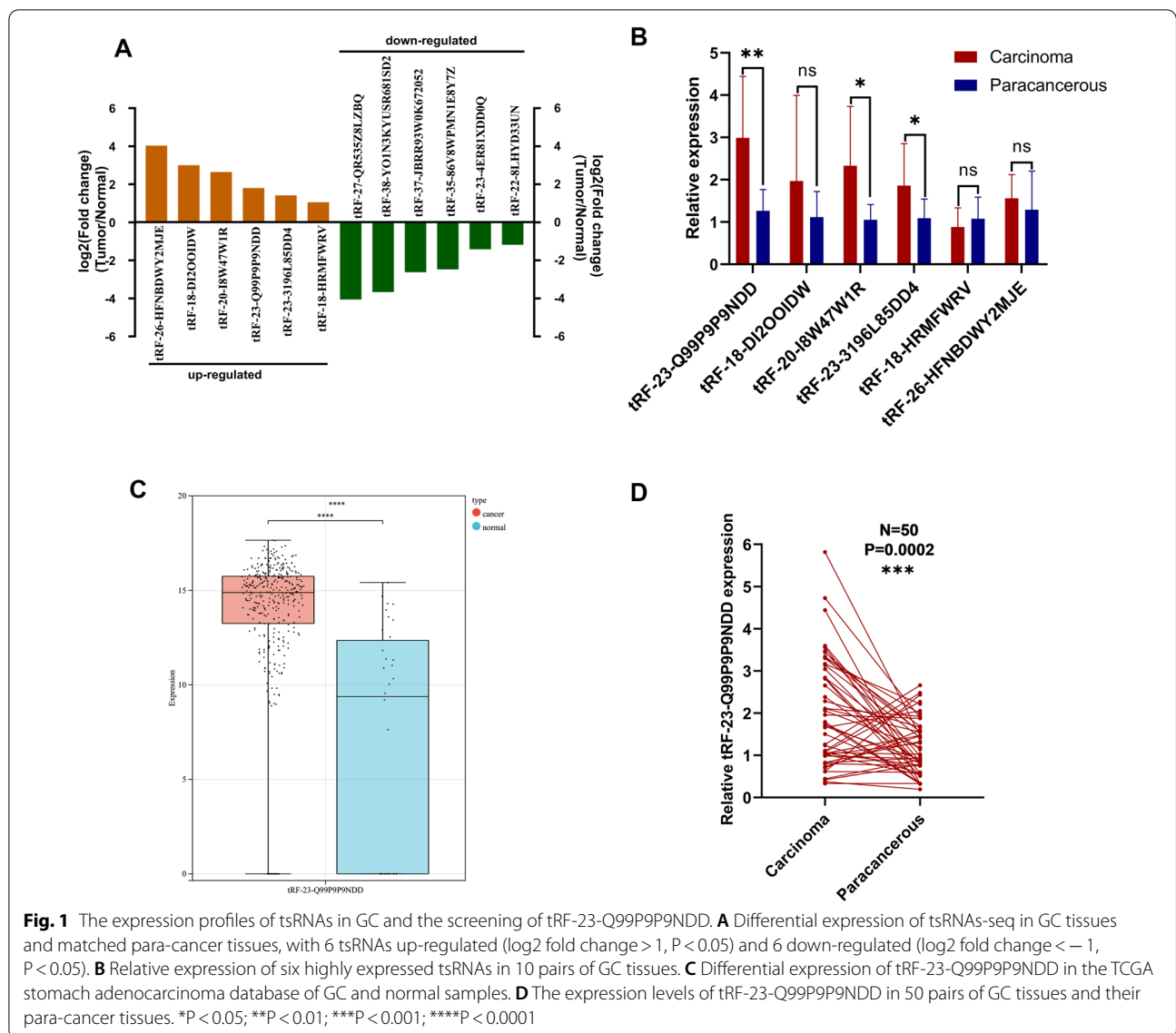


Table 1 The intra-assay CV and the inter-assay CV of tRF-23-Q99P9P9NDD

| | tRF-23-Q99P9P9NDD | U6 |
|---------------------|-------------------|------|
| Intra assay CV (%) | 1.53 | 2.17 |
| Inter assay CV, (%) | 2.29 | 2.71 |

CV coefficient of variation

tRF-23-Q99P9P9NDD, GC patients were divided into two groups: a relatively high expression group (expression level > 1.519 , $n = 62$) and a relatively low expression group (expression level ≤ 1.519 , $n = 62$), and the Chi-square test was used to evaluate the correlation between tRF-23-Q99P9P9NDD expression and clinicopathological parameters in 124 GC patients. The

result showed that the expression level of tRF-23-Q99P9P9NDD was significantly associated with T stage ($P = 0.007$), lymph node metastasis ($P = 0.001$), TNM stage ($P < 0.0001$), and nerve/vascular invasion ($P = 0.026$), but showed no significant differences with other parameters (sex, age, tumor size, differentiation grade, Lauren classification, C-erbB-2, and MMR) (Table 2), suggesting that the high expression of tRF-23-Q99P9P9NDD may have potential value in predicting the malignancy progression of tumors.

Next, the clinicopathological parameters with obvious differences were divided into groups to specifically detect the differences in expression levels of tRF-23-Q99P9P9NDD in each group. The expression level of tRF-23-Q99P9P9NDD increased with the depth

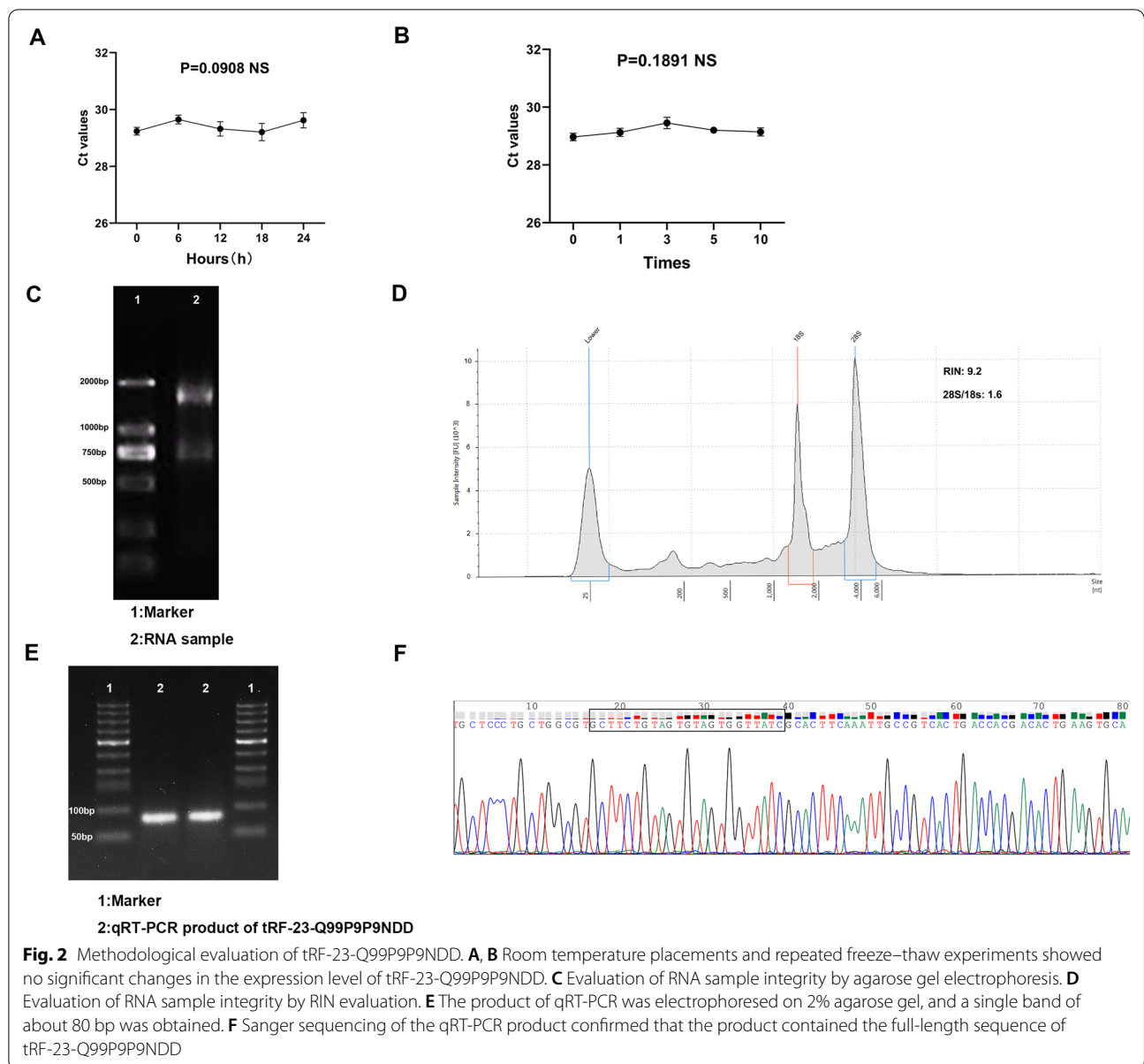
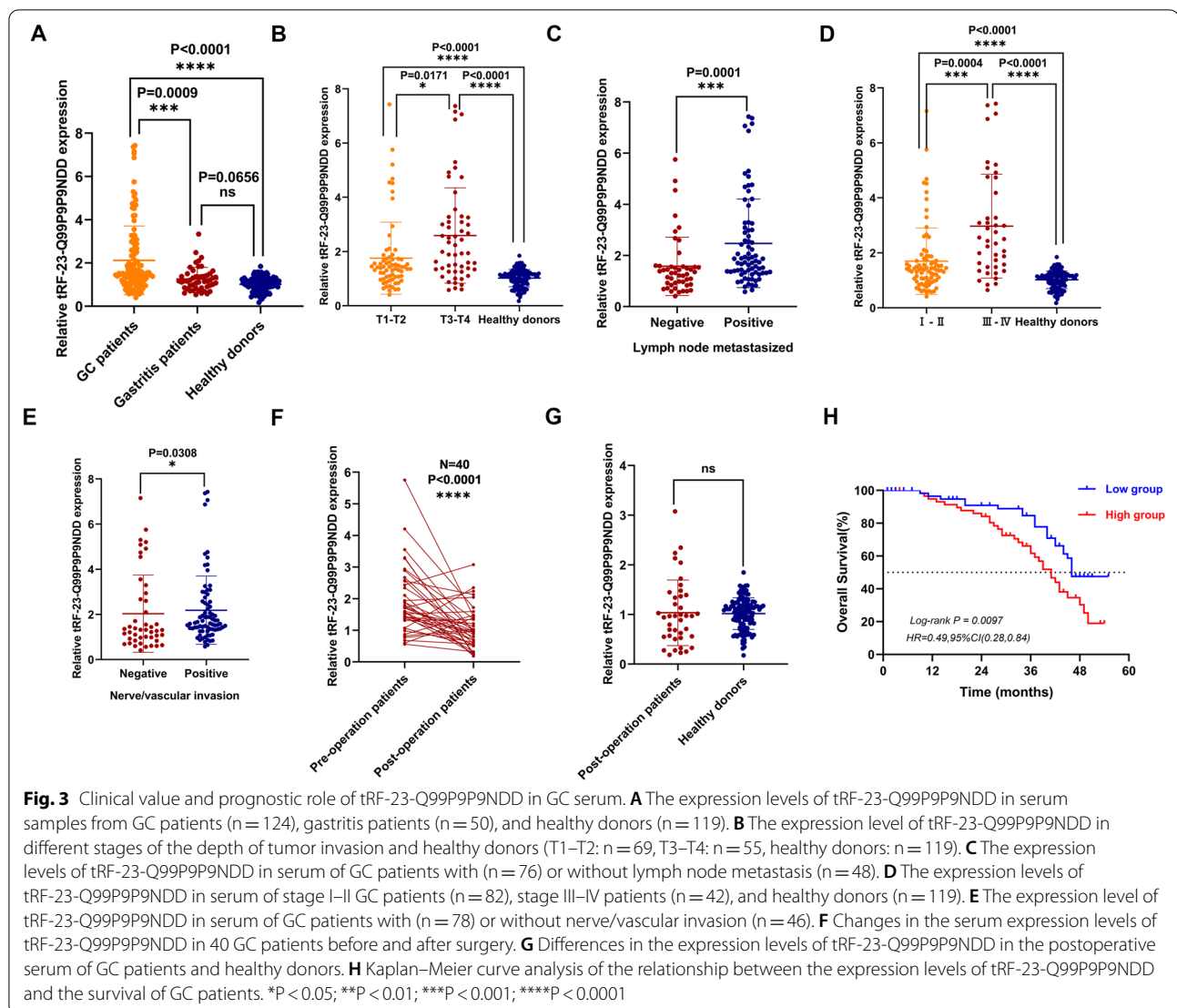


Fig. 2 Methodological evaluation of tRF-23-Q99P9P9NDD. **A, B** Room temperature placements and repeated freeze–thaw experiments showed no significant changes in the expression level of tRF-23-Q99P9P9NDD. **C** Evaluation of RNA sample integrity by agarose gel electrophoresis. **D** Evaluation of RNA sample integrity by RIN evaluation. **E** The product of qRT-PCR was electrophoresed on 2% agarose gel, and a single band of about 80 bp was obtained. **F** Sanger sequencing of the qRT-PCR product confirmed that the product contained the full-length sequence of tRF-23-Q99P9P9NDD

of tumor invasion (Fig. 3B). Moreover, lymph node metastasized GC patients had a significantly higher level of tRF-23-Q99P9P9NDD than those of the non-metastasis group (Fig. 3C). Subsequently, we analyzed the expression of tRF-23-Q99P9P9NDD in the serum of healthy donors and stage I–IV GC patients, and we found that the level of tRF-23-Q99P9P9NDD was highest in stage III–IV patients, followed by stage I–II, both of which were significantly higher than in healthy donors (Fig. 3D). Furthermore, the expression level of tRF-23-Q99P9P9NDD in serum of GC patients with nerve/vascular invasion was higher than in GC patients without invasion (Fig. 3E). To

verify whether tRF-23-Q99P9P9NDD can be a prognostic biomarker of GC, we tracked the serum tRF-23-Q99P9P9NDD expression in 40 patients with GC after surgery and found that the expression level of tRF-23-Q99P9P9NDD decreased significantly ($P < 0.0001$) (Fig. 3F) and approached a normal level after surgery ($P = 0.2873$) (Fig. 3G). Kaplan–Meier analysis showed that the low expression of the tRF-23-Q99P9P9NDD group had a higher survival rate than in the high expression group (Fig. 3H). In conclusion, we reasoned that tRF-23-Q99P9P9NDD has the potential to become a diagnostic biomarker for GC and can dynamically monitor tumor progression.



Diagnostic value of serum tRF-23-Q99P9P9NDD for GC

CEA, CA199, and CA724 are the most common biomarkers for GC. We discovered that tRF-23-Q99P9P9NDD expression was considerably higher in GC patients with $\text{CEA} \geq 5$ ng/mL than in patients with $\text{CEA} < 5$ ng/mL ($P < 0.0001$) (Fig. 4A). Furthermore, GC patients with $\text{CA199} \geq 37$ U/mL had a significantly higher level of tRF-23-Q99P9P9NDD than patients with $\text{CA199} < 37$ U/mL ($P < 0.0001$) (Fig. 4B). In addition, the tRF-23-Q99P9P9NDD level in GC patients with $\text{CA724} \geq 10$ U/mL was significantly higher than in patients with $\text{CA724} < 10$ U/mL ($P < 0.0001$) (Fig. 4C). Furthermore, the level of tRF-23-Q99P9P9NDD in GC serum was positively correlated with CEA and CA199, but not highly correlated with CA724 (Additional file 2: Fig. S2A–C). We conducted a correlation analysis between 50 GC tissues collected and serum samples of corresponding patients,

and the results indicated that patients with higher serum tRF-23-Q99P9P9NDD levels also had higher expression in the paired GC tissues (Fig. 4D).

Next, we comprehensively analyzed the diagnostic efficacy of each biomarker. We performed ROC analyses to determine the diagnostic efficacy of tRF-23-Q99P9P9NDD, CEA, CA199, and CA724 in GC. tRF-23-Q99P9P9NDD had an AUC of 0.783 (95% confidence interval (CI) 0.725–0.842), which was higher than 0.715 (95% CI 0.649–0.780) of CEA, 0.614 (95% CI 0.543–0.686) of CA199, and 0.751 (95% CI 0.690–0.812) of CA724 (Fig. 5A). Meanwhile, tRF-23-Q99P9P9NDD had 67% SEN and 86% SPE in differentiating GC patients from healthy donors when the cut-off point was 1.317150645 and the Youden index was 0.526. The SEN of CEA, CA199, and CA724 was 60%, 44%, and 53%, and the SPE was 74%, 77%, and 86%, respectively (Table 3). In

Table 2 Clinicopathological analysis of tRF-23-Q99P9P9NDD

| Parameter | | No. of patients | tRF-23-Q99P9P9NDD (high) | tRF-23-Q99P9P9NDD (low) | P-value |
|-------------------------|------------------------|-----------------|--------------------------|-------------------------|----------|
| Sex | Male | 83 | 42 | 41 | 0.849 |
| | Female | 41 | 20 | 21 | |
| Age (year) | < 60 | 39 | 18 | 21 | 0.562 |
| | ≥ 60 | 85 | 44 | 41 | |
| Tumor size | < 5 | 96 | 50 | 46 | 0.39 |
| | ≥ 5 | 28 | 12 | 16 | |
| Differentiation grade | Well-moderate | 51 | 27 | 24 | 0.584 |
| | Poor-undifferentiation | 73 | 35 | 38 | |
| T stage | T1-T2 | 69 | 27 | 42 | 0.007 |
| | T3-T4 | 55 | 35 | 20 | |
| Lymph node metastasis | Positive | 76 | 47 | 29 | 0.001 |
| | Negative | 48 | 15 | 33 | |
| TNM stage | I-II | 82 | 31 | 51 | < 0.0001 |
| | III-IV | 42 | 31 | 11 | |
| Nerve/vascular invasion | Positive | 78 | 45 | 33 | 0.026 |
| | Negative | 46 | 17 | 29 | |
| Lauren classification | Intestinal type | 34 | 16 | 18 | 0.54 |
| | Mixed type | 38 | 17 | 21 | |
| | Diffuse type | 52 | 29 | 23 | |
| C-erbB-2 | Positive | 7 | 3 | 4 | 0.697 |
| | Negative | 117 | 59 | 58 | |
| MMR | dMMR | 3 | 2 | 1 | 0.559 |
| | pMMR | 121 | 60 | 61 | |

MLH1, PMS2, MSH2, and MSH6 were all positive for pMMR (normal expression), and 1 or more negative for dMMR (deletion)

addition, the overall accuracy (ACCU), positive predictive value (PPV), and negative predictive value (NPV) of tRF-23-Q99P9P9NDD were as follows: 76%, 83%, and 71%, which were higher than those of CEA, CA199, and CA724. Thus, tRF-23-Q99P9P9NDD demonstrated better diagnostic efficacy than other GC biomarkers when diagnosed alone. Next, tRF-23-Q99P9P9NDD was combined with CEA, CA199, and CA724, as well as the combination of the three and four biomarkers (Fig. 5B, C Additional file 3: Table S1). It was found that the AUC of combined diagnosis was higher than any single biomarker; moreover, the AUC reached the highest value of 0.862, and the SEN also reached the highest value of 83% in the combination of the four biomarkers (Table 3). In conclusion, tRF-23-Q99P9P9NDD may be a potential GC biomarker, and the diagnostic efficacy of a single marker can be improved by the combination of biomarkers.

Due to the low SEN of clinical biomarkers, most GC patients are already at an intermediate to an advanced stage by the time they are diagnosed, missing the best chance for early treatment. We collected the information from 82 early GC patients (stages I and II) and 119 healthy donors for evaluation. The ROC curves showed

that the AUC of tRF-23-Q99P9P9NDD was 0.724 (95% CI 0.648–0.800), which was better than 0.664 (95% CI 0.584–0.743) of CEA, 0.590 (95% CI 0.506–0.673) of CA199, and 0.711 (95% CI 0.636–0.787) of CA724 (Fig. 5D). In addition, the SEN of tRF-23-Q99P9P9NDD was 60%, the SPE was 85% when the cut-off point was 1.309670707, and the Youden index was 0.446, and the ACCU, PPV, and NPV were 75%, 73%, and 75%, respectively, which were all higher than those of CEA, CA199, and CA724. It was satisfactory that the AUC of combined diagnosis was higher than that of a single biomarker in identifying early GC patients and healthy donors (Fig. 5E, F, Additional file 4: Table S2). The AUC reached the highest when the four were combined, which was 0.819, and the SEN increased to 78% (Table 4). The above findings indicate the potential value of tRF-23-Q99P9P9NDD for the early diagnosis of GC.

It is well known that GC may be transformed from chronic gastritis (Sipponen and Maaros 2015), and in this study, the expression levels of tRF-23-Q99P9P9NDD in the serum of GC and gastritis patients are different. Thus, we performed a ROC analysis on the data of 124 GC patients and 50 gastritis patients, and we discovered

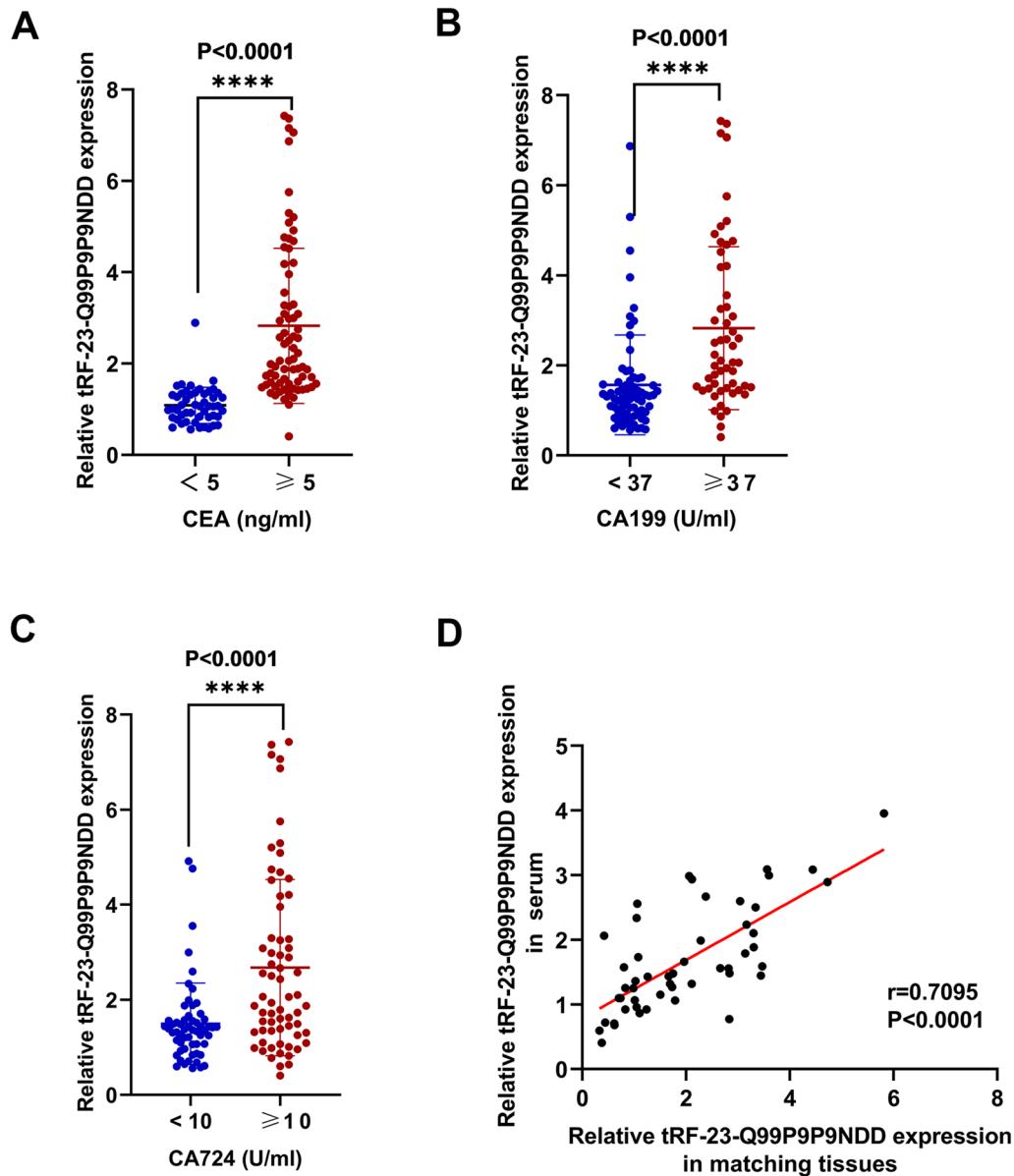


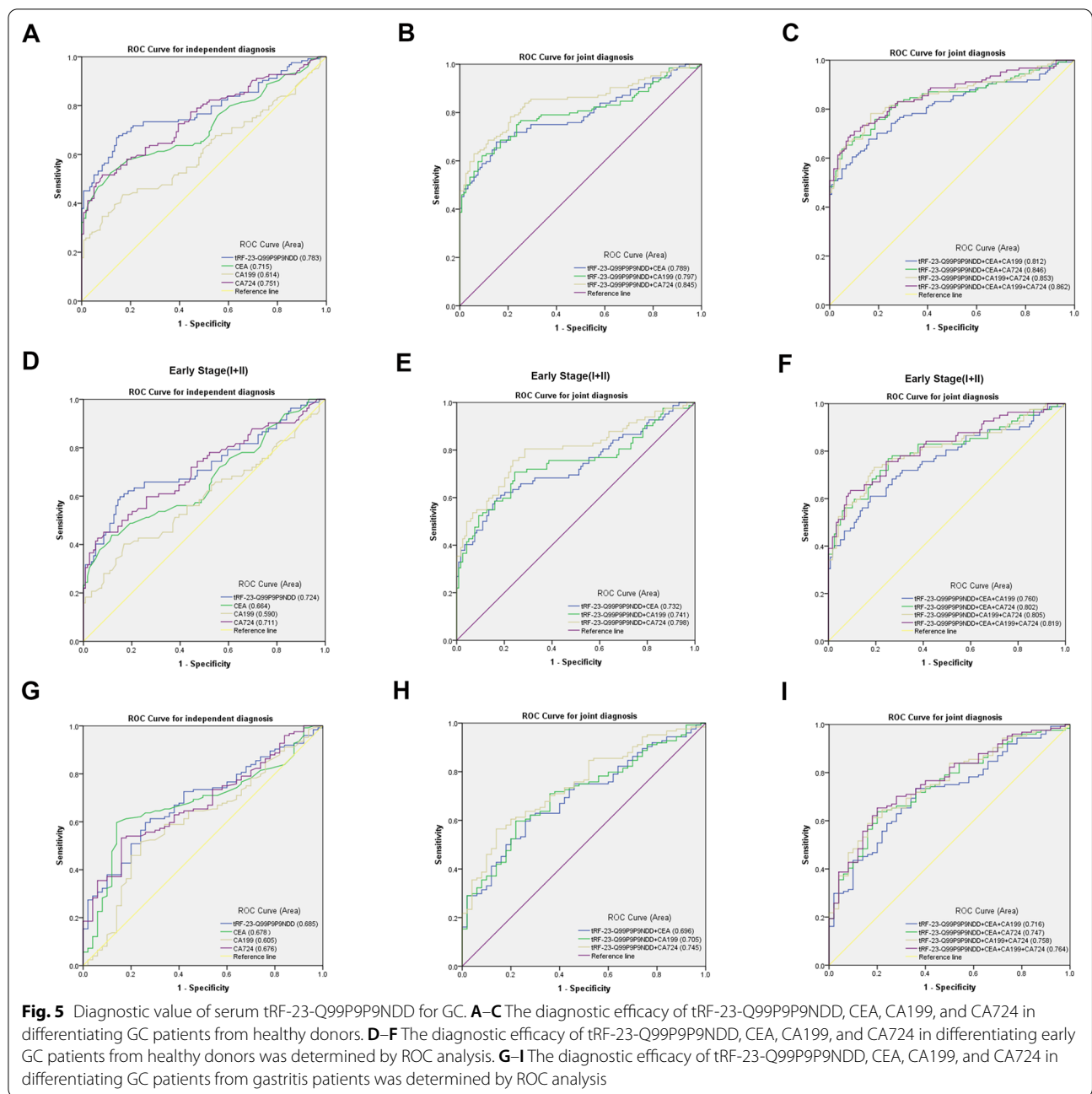
Fig. 4 The relationship between the expression levels of serum tRF-23-Q99P9P9NDD and conventional biomarkers of GC. **A–C** GC patients were divided into two groups according to the diagnostic thresholds of CEA, CA199, and CA724, and the expression level of tRF-23-Q99P9P9NDD was analyzed respectively. **D** Pearson correlation analysis was performed on tRF-23-Q99P9P9NDD expression levels in 50 GC tissues and serum samples from corresponding patients. *P < 0.05; **P < 0.01; ***P < 0.001; ****P < 0.0001

that the AUC of tRF-23-Q99P9P9NDD was 0.685 (95% CI 0.605–0.766), which was higher than the 0.678 (95% CI 0.594–0.761) for CEA, 0.605 (95% CI 0.512–0.697) for CA199, and 0.676 (95% CI 0.594–0.757) for CA724 (Fig. 5G). tRF-23-Q99P9P9NDD had 60% SEN and 74% SPE in differentiating GC patients from healthy donors when the cut-off point was 1.391759517 and the Youden index was 0.337. When tRF-23-Q99P9P9NDD was combined with other biomarkers, the AUC increased,

reaching the highest AUC of 0.764 (95% CI 0.690–0.837) when all four biomarkers were combined (Fig. 5H, I, Additional file 5: Table S3), and the SEN increased to 81% (Table 5).

Prediction of tRF-23-Q99P9P9NDD downstream in GC cells

The cellular localization of tRF-23-Q99P9P9NDD was detected by nuclear and cytoplasmic RNA separation assays, showing that tRF-23-Q99P9P9NDD was mainly



located in the nucleus, which provided some ideas for our future experiments (Fig. 6A). Because the function of tRF-23-Q99P9NDD may be similar to that of miRNAs, we used bioinformatics database analysis (miRanda, RNAhybrid, TargetScan) to predict the potential mechanism of tsRNAs-mRNA regulatory axis in GC. The connection network showed 100 targeted genes corresponding to tRF-23-Q99P9NDD (Fig. 6B). Subsequently, we verified the expression levels of three potential target genes (*BCKDHB*, *DGKD*,

and *GNPDA2*) in GC cell lines (Fig. 6C–E). After transfection of tRF-23-Q99P9NDD mimics and mimics NC into AGS and MKN-45, the expression trends of these three target genes were verified (Fig. 6F). These results indicated that tRF-23-Q99P9NDD may play an important role in the occurrence and development of GC by targeting downstream mRNA, which provides a new direction for further exploration of specific molecular mechanisms of tRF-23-Q99P9NDD in GC.

Table 3 The diagnostic performance of tRF-23-Q99P9P9NDD, CEA, CA199 and CA724 in differentiating GC patients from healthy donors

| | SEN (%) | SPE (%) | ACCU (%) | PPV (%) | NPV (%) |
|---|----------------|----------------|----------------|----------------|----------------|
| tRF-23-Q99P9P9NDD | 0.67 (83/124) | 0.86 (102/119) | 0.76 (185/243) | 0.83 (83/100) | 0.71 (102/143) |
| CEA | 0.60 (74/124) | 0.74 (88/119) | 0.67 (162/243) | 0.70 (74/105) | 0.64 (88/138) |
| CA199 | 0.44 (55/124) | 0.77 (92/119) | 0.60 (147/243) | 0.67 (55/82) | 0.57 (92/161) |
| CA724 | 0.53 (66/124) | 0.86 (102/119) | 0.69 (168/243) | 0.80 (66/83) | 0.64 (102/160) |
| tRF-23-Q99P9P9NDD + CEA | 0.71 (88/124) | 0.65 (77/119) | 0.68 (165/243) | 0.68 (88/130) | 0.68 (77/113) |
| tRF-23-Q99P9P9NDD + CA199 | 0.73 (90/124) | 0.73 (87/119) | 0.73 (177/243) | 0.74 (90/122) | 0.72 (87/121) |
| tRF-23-Q99P9P9NDD + CA724 | 0.80 (99/124) | 0.76 (90/119) | 0.78 (189/243) | 0.77 (99/128) | 0.78 (90/115) |
| tRF-23-Q99P9P9NDD + CEA + CA199 | 0.75 (93/124) | 0.56 (67/119) | 0.66 (160/243) | 0.64 (93/145) | 0.68 (67/98) |
| tRF-23-Q99P9P9NDD + CEA + CA724 | 0.81 (101/124) | 0.56 (67/119) | 0.69 (168/243) | 0.66 (101/153) | 0.74 (67/90) |
| tRF-23-Q99P9P9NDD + CEA + CA199 + CA724 | 0.83 (103/124) | 0.49 (58/119) | 0.66 (161/243) | 0.63 (103/164) | 0.73 (58/79) |

SEN sensitivity; SPE specificity; ACCU overall accuracy; PPV positive predictive value; NPV negative predictive value

Table 4 The diagnostic performance of tRF-23-Q99P9P9NDD, CEA, CA199 and CA724 in differentiating early GC patients from healthy donors

| | SEN (%) | SPE (%) | ACCU (%) | PPV (%) | NPV (%) |
|---|--------------|----------------|----------------|---------------|----------------|
| tRF-23-Q99P9P9NDD | 0.60 (49/82) | 0.85 (101/119) | 0.75 (150/201) | 0.73 (49/67) | 0.75 (101/134) |
| CEA | 0.51 (42/82) | 0.74 (88/119) | 0.65 (130/201) | 0.58 (42/73) | 0.69 (88/128) |
| CA199 | 0.41 (34/82) | 0.77 (92/119) | 0.63 (126/201) | 0.56 (34/61) | 0.66 (92/140) |
| CA724 | 0.46 (38/82) | 0.86 (102/119) | 0.70 (140/201) | 0.69 (38/55) | 0.70 (102/146) |
| tRF-23-Q99P9P9NDD + CEA | 0.65 (53/82) | 0.64 (76/119) | 0.64 (129/201) | 0.55 (53/96) | 0.72 (76/105) |
| tRF-23-Q99P9P9NDD + CA199 | 0.66 (54/82) | 0.72 (86/119) | 0.70 (140/201) | 0.62 (54/87) | 0.75 (86/114) |
| tRF-23-Q99P9P9NDD + CA724 | 0.74 (61/82) | 0.75 (89/119) | 0.75 (150/201) | 0.67 (61/91) | 0.81 (89/110) |
| tRF-23-Q99P9P9NDD + CEA + CA199 | 0.68 (56/82) | 0.55 (66/119) | 0.61 (122/201) | 0.51 (56/109) | 0.72 (66/92) |
| tRF-23-Q99P9P9NDD + CEA + CA724 | 0.77 (63/82) | 0.55 (66/119) | 0.64 (129/201) | 0.54 (63/116) | 0.78 (66/85) |
| tRF-23-Q99P9P9NDD + CEA + CA199 + CA724 | 0.78 (64/82) | 0.48 (57/119) | 0.60 (121/201) | 0.51 (64/126) | 0.76 (57/75) |

SEN sensitivity; SPE specificity; ACCU overall accuracy; PPV positive predictive value; NPV negative predictive value

Table 5 The diagnostic performance of tRF-23-Q99P9P9NDD, CEA, CA199 and CA724 in differentiating GC patients from gastritis patients

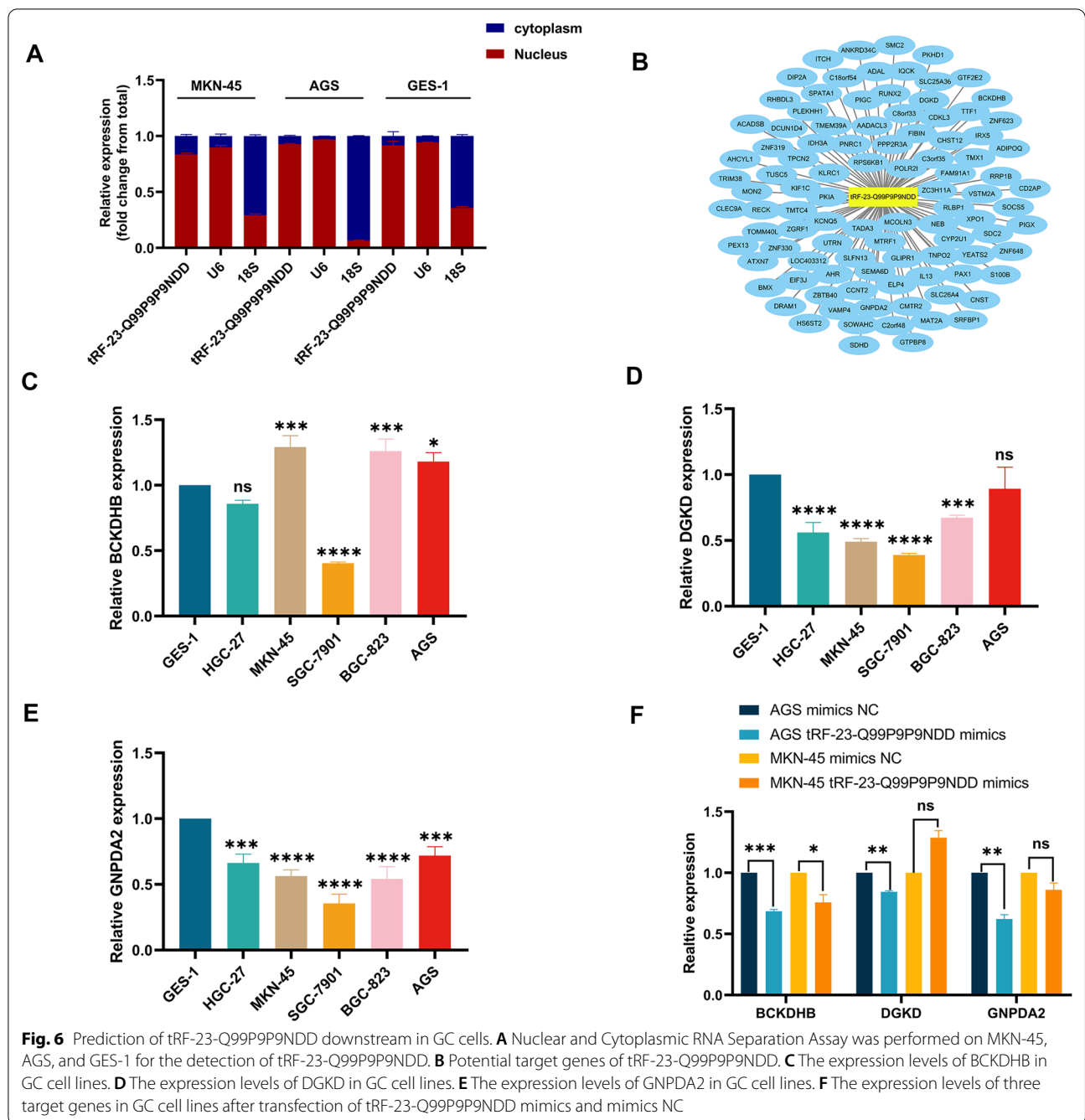
| | SEN (%) | SPE (%) | ACCU (%) | PPV (%) | NPV (%) |
|---|----------------|--------------|----------------|----------------|---------------|
| tRF-23-Q99P9P9NDD | 0.60 (74/124) | 0.74 (37/50) | 0.64 (111/174) | 0.85 (74/87) | 0.43 (37/87) |
| CEA | 0.60 (74/124) | 0.86 (43/50) | 0.67 (117/174) | 0.91 (74/81) | 0.46 (43/93) |
| CA199 | 0.44 (55/124) | 0.80 (40/50) | 0.55 (95/174) | 0.85 (55/65) | 0.37 (40/109) |
| CA724 | 0.53 (66/124) | 0.84 (42/50) | 0.62 (108/174) | 0.89 (66/74) | 0.42 (42/100) |
| tRF-23-Q99P9P9NDD + CEA | 0.66 (82/124) | 0.68 (34/50) | 0.67 (116/174) | 0.84 (82/98) | 0.45 (34/76) |
| tRF-23-Q99P9P9NDD + CA199 | 0.67 (83/124) | 0.60 (30/50) | 0.65 (113/174) | 0.81 (83/103) | 0.42 (30/71) |
| tRF-23-Q99P9P9NDD + CA724 | 0.76 (94/124) | 0.66 (33/50) | 0.73 (127/174) | 0.85 (94/111) | 0.52 (33/63) |
| tRF-23-Q99P9P9NDD + CEA + CA199 | 0.70 (87/124) | 0.56 (28/50) | 0.66 (115/174) | 0.80 (87/109) | 0.43 (28/65) |
| tRF-23-Q99P9P9NDD + CEA + CA724 | 0.80 (99/124) | 0.60 (30/50) | 0.74 (129/174) | 0.83 (99/119) | 0.55 (30/55) |
| tRF-23-Q99P9P9NDD + CEA + CA199 + CA724 | 0.81 (101/124) | 0.48 (24/50) | 0.72 (125/174) | 0.80 (101/127) | 0.51 (24/47) |

SEN sensitivity; SPE specificity; ACCU overall accuracy; PPV positive predictive value; NPV negative predictive value

Discussion

GC is one of the most critical cancers in the world. Although surgical techniques, radiotherapy, and

chemotherapy drugs have progressed, the morbidity and mortality of GC still rank fifth and fourth worldwide, respectively (Tan 2019; Sung et al. 2021). Early



GC patients usually have no apparent symptoms, and 80% of GC patients are at the late stage when diagnosed, which leads to their missed opportunity for radical resection (Wang et al. 2019). However, because the SEN and SPE of existing clinical tumor biomarkers are not high enough (Wu et al. 2014), we need to find new biomarkers to improve the early diagnosis value of GC. With the development of high-throughput sequencing technology, it has been found that the analysis of differential gene

expression can help discover potential cancer biomarkers and advance human research on the mechanism of tumor disease (Govindarajan et al. 2020; Hong et al. 2020).

Through high-throughput sequencing, the gene regulatory role of ncRNA in cancer has been further revealed, and its application as a cancer biomarker has gradually become widespread (Esteller 2011; Sun and Chen 2020). However, the existing tumor biomarkers still have certain limitations. Therefore, researchers still keep finding more

efficient tumor biomarkers. When short RNAs less than 40 nt in length for research were selected, it was discovered that many sequencing reads were mapped to RNA fragments produced by the cleavage of tRNA transcripts, known as tsRNAs (Romano et al. 2017). tsRNAs are a new class of small ncRNA produced by enzymatic cleavage of tRNAs and are stably present with specific biological functions in serum, saliva, and extracellular vesicles, among other locations (Dhahbi et al. 2013; Anderson and Ivanov 2014; Chiou et al. 2018; Li et al. 2018; Sun and Chen 2020). More and more cases of abnormal tsRNAs expression in cancer have been discovered. In non-small cell lung cancer, for example, tRF-Leu-CAG is highly elevated (Shao et al. 2017). Similarly, patients with liver cancer have much higher levels of tRF-5^{GluCTC} in their plasma exosomes than healthy donors, which can be a new biomarker for diagnosing liver cancer (Zhu et al. 2019a, b). In this study, tRF-23-Q99P9P9NDD with high expression in GC was screened out by high-throughput sequencing. To explore the diagnostic value of tRF-23-Q99P9P9NDD in GC, we expanded the sample size for verification. The results showed that tRF-23-Q99P9P9NDD expression in GC serum was indeed higher than in gastritis patients and healthy donors, which could clearly distinguish GC patients from gastritis patients and healthy donors. Perhaps more promisingly, tsRNAs could also be used to monitor disease progression, not just for the diagnosis. We found that the expression level of serum tRF-23-Q99P9P9NDD was significantly decreased after surgery. In addition, analysis of clinicopathological parameters indicated that the expression level of tRF-23-Q99P9P9NDD was positively associated with T stage, lymph node metastasis, TNM stage, and nerve/vascular invasion, implying that it could be a potential GC therapeutic target. According to the Kaplan–Meier analysis, decreased expression group was associated with a more prolonged overall survival. All of these studies indicated that tRF-23-Q99P9P9NDD has great promise as a clinical biomarker for GC diagnosis and prognosis.

Through different regulatory mechanisms, tsRNAs can influence the process of tumorigenesis and progression (Anderson and Ivanov 2014; Schimmel 2018; Zhu et al. 2019a, b; Yu et al. 2020). For example, Xu et al. established that tRF-Glu-TTC-027 could inhibit the progress of GC by inhibiting the MAPK signaling pathway (Xu et al. 2021). By targeting FBXO47, Zhang et al. found that tRF-3019a promoted GC cell proliferation, migration, and invasion (Zhang et al. 2020). They focused on exploring the regulatory mechanism of tsRNAs in cancer, and only briefly described the expression of molecules and preliminarily evaluated the diagnostic efficacy without specifically analyzing the diagnostic value of tsRNAs

as tumor markers. This study explored the potential of tRF-23-Q99P9P9NDD as a GC biomarker for the first time. First, we evaluated the detection method of tRF-23-Q99P9P9NDD and found that its performance was relatively stable, which shows promise for clinical application. Next, we comprehensively analyzed the diagnostic efficacy of tRF-23-Q99P9P9NDD, and we found that the difference in the expression level of serum tRF-23-Q99P9P9NDD could help us identify GC patients and monitor GC progression. Importantly, when we compared tRF-23-Q99P9P9NDD with the clinical GC biomarkers CEA, CA199, and CA724 by ROC, we found that tRF-23-Q99P9P9NDD had higher diagnostic efficiency than other biomarkers, and the combination further improved the diagnostic efficiency. A point of caution is that many current biomarkers are not easily detected in the early stages; they are usually detected in the late stages of GC (Necula et al. 2019). Therefore, we evaluated the diagnostic efficacy of tRF-23-Q99P9P9NDD in the early stages (stages I and II). It is satisfactory that the AUC and sensitivity of tRF-23-Q99P9P9NDD were higher than those of clinical common biomarkers. Thus, tRF-23-Q99P9P9NDD can better distinguish early GC from healthy donors, and a new strategy for early GC diagnosis based on this biomarker should be developed soon. However, our samples did not cover multiple regional specimens due to the limited conditions. The experimental results may not be representative and the sample size still needs to be supplemented. Next, we will continue to collect specimens and data for further analysis to confirm the diagnostic efficiency of tRF-23-Q99P9P9NDD in GC.

Although some progress has been made in our study, the underlying mechanism of differential expression of tRF-23-Q99P9P9NDD remains unclear. With the proliferation of tumor cells, local tumor cells are in a hypoxia state. Tao et al. found that under the regulation of the hypoxia-inducible factor 1 subunit alpha (HIF1 α)/ANG axis, 5'tRNA-His-GTG increased, which promotes the proliferation of colorectal cancer cells by inhibiting the Hippo signaling pathway (Tao et al. 2021). In addition, Cui et al. demonstrated that hypoxia-induced tsRNAs also play an essential role in breast cancer (Goodarzi et al. 2015; Cui et al. 2019). Therefore, it is reasonable to speculate that the generation of tRF-23-Q99P9P9NDD is associated with a hypoxic environment. Furthermore, in this study, we found that tRF-23-Q99P9P9NDD belongs to 5'tRF, which is consistent with the analysis of Kumar et al. thus indicating that 5'tRF mainly exists in the nucleus (Kumar et al. 2016). According to previous studies, tsRNAs may promote or inhibit cancer through different internal mechanisms. Therefore, we speculated that tRF-23-Q99P9P9NDD might be

involved in post-transcriptional regulation through a miRNA-like role, promoting GC progression (Sun et al. 2018; Yu et al. 2021). Then, we predicted the potential target genes of tRF-23-Q99P9P9NDD through the database and preliminarily addressed the mechanism.

Conclusions

We concluded, for the first time, that tRF-23-Q99P9P9NDD is highly expressed in GC cells, tissues, and serum, and it may serve as a potential biomarker for GC. tRF-23-Q99P9P9NDD has higher diagnostic efficacy than conventional biomarkers even in the early stage. Meanwhile, the expression of tRF-23-Q99P9P9NDD was correlated with the progression of GC. We will further study the mechanism of tRF-23-Q99P9P9NDD in GC in the future.

Abbreviations

GC: Gastric cancer; CEA: Carcinoembryonic antigen; CA199: Carbohydrate antigen 199; CA724: Carbohydrate antigen 724; lncRNAs: Long non-coding RNAs; circRNAs: Circular RNAs; piRNAs: Piwi-interacting RNAs; miRNAs: MicroRNAs; tsRNAs: tRNA-derived small RNAs; tRFs: tRNA-derived fragments; tiRNAs: tRNA halves; nt: Nucleotides; ANG: Angiogenin; RISC: RNA-induced silencing complex; PUS7: Pseudouridylation synthase 7; qRT-PCR: Quantitative real-time PCR; ROC: Receiver operating characteristic curve; SD: Standard deviation; AUC: Area under curve; SEN: Sensitivity; SPE: Specificity; AGE: Agarose gel electrophoresis; CV: Coefficient of variation; CI: Confidence interval; ACCU: The overall accuracy; PPV: Positive predictive value; NPV: Negative predictive value.

Supplementary Information

The online version contains supplementary material available at <https://doi.org/10.1186/s10020-022-00491-8>.

Additional file 1: Fig. S1. tRF-23-Q99P9P9NDD is a sort of tRFs. **A** UCSC Genome Browser database showed that tRF-23-Q99P9P9NDD was located on chromosome 6p22.1 with coordinates 27,248,099–27,248,121. **B** InMINTbase v2.0, tRF-23-Q99P9P9NDD is a 5'tRF (GCTCTGTAGTGTAG TGGTTATC) with length of 23nt. **C** OncotRF database showed that the cleavage site was located on the D-loop. **D** Amplification curves of tRF-23-Q99P9P9NDD. **E** Melting curves of tRF-23-Q99P9P9NDD.

Additional file 2: Fig. S2. The correlation analysis between the expression levels of serum tRF-23-Q99P9P9NDD and conventional biomarkers of GC. **A-C** Pearson correlation analysis was performed on the expression level of tRF-23-Q99P9P9NDD and the levels of CEA, CA199, and CA724 in GC serum.

Additional file 3: Table S1. ROC analysis of all biomarkers in distinguishing GC patients from healthy donors.

Additional file 4: Table S2. ROC analysis of all biomarkers in distinguishing early GC patients from healthy donors.

Additional file 5: Table S3. ROC analysis of all biomarkers in distinguishing GC patients from gastritis patients.

Acknowledgements

We appreciate all the patients who participated in this study and all those who contributed to it. We thank LetPub (www.letpub.com) for its linguistic assistance with this manuscript.

Author contributions

ZY and GXL performed study design, material preparation, data collection and analysis. ZY written the first draft of the manuscript, QXY took part in the experiment, HYJ and JSQ provided resources and guidance for the paper, and all authors read and approved this manuscript.

Funding

This project was supported by Grants from the National Natural Science Foundation of China (Grant Nos. 81871720, 82072363) and Nantong Municipal Health Commission (Grant No. QA2020027).

Availability of data and materials

Data are available upon reasonable request. The data used in the current study are available from the corresponding author on reasonable request.

Declarations

Ethics approval and consent to participate

The ethics committee of the local hospital (ethical review report number: 2018-L055) approved the study.

Consent for publication

The informed consent obtained from study participants.

Competing interests

The authors declare that they have no competing interests.

Author details

¹Medical School of Nantong University, Nantong University, Nantong, China. ²Department of Laboratory Medicine, Affiliated Hospital of Nantong University, Xisi Road, No. 20, Nantong, China. ³Research Center of Clinical Medicine, Affiliated Hospital of Nantong University, Nantong, China. ⁴Department of Medical Oncology, Affiliated Hospital of Nantong University, Xisi Road, No. 20, Nantong, China.

Received: 23 February 2022 Accepted: 25 May 2022

Published online: 11 June 2022

References

- Anderson P, Ivanov P. tRNA fragments in human health and disease. *FEBS Lett.* 2014;588(23):4297–304.
- Chao Y, Zhou D. lncRNA-D16366 is a potential biomarker for diagnosis and prognosis of hepatocellular carcinoma. *Med Sci Monit.* 2019;25:6581–6.
- Chen Q, Yan M, Cao Z, Li X, Zhang Y, Shi J, et al. Sperm tsRNAs contribute to intergenerational inheritance of an acquired metabolic disorder. *Science.* 2016;351(6271):397–400.
- Chiou NT, Kageyama R, Ansel KM. Selective export into extracellular vesicles and function of tRNA fragments during T cell activation. *Cell Rep.* 2018;25(12):3356–3370.e3354.
- Cui Y, Huang Y, Wu X, Zheng M, Xia Y, Fu Z, et al. Hypoxia-induced tRNA-derived fragments, novel regulatory factor for doxorubicin resistance in triple-negative breast cancer. *J Cell Physiol.* 2019;234(6):8740–51.
- Dassen AE, Lemmens VE, van de Poll-Franse LV, Creemers GJ, Brenninkmeijer SJ, Lips DJ, et al. Trends in incidence, treatment and survival of gastric adenocarcinoma between 1990 and 2007: a population-based study in the Netherlands. *Eur J Cancer (Oxford, England: 1990).* 2010;46(6):1101–10.
- den Hoed CM, Kuipers EJ. Gastric cancer: how can we reduce the incidence of this disease? *Curr Gastroenterol Rep.* 2016;18(7):34.
- Dhabhi JM, Spindler SR, Atamna H, Yamakawa A, Boffelli D, Mote P, et al. 5' tRNA halves are present as abundant complexes in serum, concentrated in blood cells, and modulated by aging and calorie restriction. *BMC Genomics.* 2013;14:298.
- Esteller M. Non-coding RNAs in human disease. *Nat Rev Genet.* 2011;12(12):861–74.
- Goodarzi H, Liu X, Nguyen HC, Zhang S, Fish L, Tavazoie SF. Endogenous tRNA-derived fragments suppress breast cancer progression via YBX1 displacement. *Cell.* 2015;161(4):790–802.

- Govindarajan M, Wohlmuth C, Waas M, Bernardini MQ, Kislinger T. High-throughput approaches for precision medicine in high-grade serous ovarian cancer. *J Hematol Oncol*. 2020;13(1):134.
- Gu XL, Ma S, Liang B, Ju SQ. Serum hsa_tsr016141 as a kind of tRNA-derived fragments is a novel biomarker in gastric cancer. *Front Oncol*. 2021;11:8.
- Guzzi N, Cieřla M, Ngoc PCT, Lang S, Arora S, Dimitriou M, et al. Pseudouridylation of tRNA-derived fragments steers translational control in stem cells. *Cell*. 2018;173(5):1204–1216.e1226.
- Hong M, Tao S, Zhang L, Diao LT, Huang X, Huang S, et al. RNA sequencing: new technologies and applications in cancer research. *J Hematol Oncol*. 2020;13(1):166.
- Kalniņa Z, Meistere I, Kikuste I, Tolmanis I, Zayakin P, Linē A. Emerging blood-based biomarkers for detection of gastric cancer. *World J Gastroenterol*. 2015;21(41):11636–53.
- Kumar P, Kuscu C, Dutta A. Biogenesis and function of transfer RNA-related fragments (tRFs). *Trends Biochem Sci*. 2016;41(8):679–89.
- Li P-F, Chen S-C, Xia T, Jiang X-M, Shao Y-F, Xiao B-X, et al. Non-coding RNAs and gastric cancer. *World J Gastroenterol*. 2014;20(18):5411–9.
- Li F, Kaczor-Urbanowicz KE, Sun J, Majem B, Lo HC, Kim Y, et al. Characterization of human salivary extracellular RNA by next-generation sequencing. *Clin Chem*. 2018;64(7):1085–95.
- Mo D, Jiang P, Yang Y, Mao X, Tan X, Tang X, et al. A tRNA fragment, 5'-tiRNA (Val), suppresses the Wnt/ β -catenin signaling pathway by targeting FZD3 in breast cancer. *Cancer Lett*. 2019;457:60–73.
- Necula L, Matei L, Dragu D, Neagu AI, Mambet C, Nedeianu S, et al. Recent advances in gastric cancer early diagnosis. *World J Gastroenterol*. 2019;25(17):2029–44.
- Park JY, von Karsa L, Herrero R. Prevention strategies for gastric cancer: a global perspective. *Clin Endosc*. 2014;47(6):478–89.
- Piazuelo MB, Correa P. Gastric cancer: overview. *Colombia Medica*. 2013;44(3):192–201.
- Romano G, Veneziano D, Acunzo M, Croce CM. Small non-coding RNA and cancer. *Carcinogenesis*. 2017;38(5):485–91.
- Schimmel P. The emerging complexity of the tRNA world: mammalian tRNAs beyond protein synthesis. *Nat Rev Mol Cell Biol*. 2018;19(1):45–58.
- Shao Y, Sun Q, Liu X, Wang P, Wu R, Ma Z. tRF-Leu-CAG promotes cell proliferation and cell cycle in non-small cell lung cancer. *Chem Biol Drug Des*. 2017;90(5):730–8.
- Shimada H, Noie T, Ohashi M, Oba K, Takahashi Y. Clinical significance of serum tumor markers for gastric cancer: a systematic review of literature by the Task Force of the Japanese Gastric Cancer Association. *Gastric Cancer*. 2014;17(1):26–33.
- Sipponen P, Maarros H. Chronic gastritis. *Scand J Gastroenterol*. 2015;50(6):657–67.
- Sun YM, Chen YQ. Principles and innovative technologies for decrypting noncoding RNAs: from discovery and functional prediction to clinical application. *J Hematol Oncol*. 2020;13(1):109.
- Sun C, Fu Z, Wang S, Li J, Li Y, Zhang Y, et al. Roles of tRNA-derived fragments in human cancers. *Cancer Lett*. 2018;414:16–25.
- Sung H, Ferlay J, Siegel RL, Laversanne M, Soerjomataram I, Jemal A, et al. Global cancer statistics 2020: GLOBOCAN estimates of incidence and mortality worldwide for 36 cancers in 185 countries. *CA*. 2021;71(3):209–49.
- Tan Z. Recent advances in the surgical treatment of advanced gastric cancer: a review. *Med Sci Monit*. 2019;25:3537–41.
- Tao EW, Wang HL, Cheng WY, Liu QQ, Chen YX, Gao QY. A specific tRNA half, 5'-tiRNA-His-GTG, responds to hypoxia via the HIF1 α /ANG axis and promotes colorectal cancer progression by regulating LATS2. *J Exp Clin Cancer Res*. 2021;40(1):67.
- Tong L, Zhang W, Qu B, Zhang F, Wu Z, Shi J, et al. The tRNA-derived fragment-3017A promotes metastasis by inhibiting NELL2 in human gastric cancer. *Front Oncol*. 2020;10:570916.
- Wang FH, Shen L, Li J, Zhou ZW, Liang H, Zhang XT, et al. The Chinese Society of Clinical Oncology (CSCO): clinical guidelines for the diagnosis and treatment of gastric cancer. *Cancer Commun*. 2019;39:1–31.
- Wang YZ, Li Z, Xu SY, Guo JM. Novel potential tumor biomarkers: Circular RNAs and exosomal circular RNAs in gastrointestinal malignancies. *J Clin Lab Anal*. 2020;34(7):23359.
- Wang J, Ma G, Ge H, Han X, Mao X, Wang X, et al. Circulating tRNA-derived small RNAs (tsRNAs) signature for the diagnosis and prognosis of breast cancer. *NPJ Breast Cancer*. 2021;7(1):4.
- Wu HH, Lin WC, Tsai KW. Advances in molecular biomarkers for gastric cancer: miRNAs as emerging novel cancer markers. *Expert Rev Mol Med*. 2014;16:e1.
- Wu J-Y, Lee Y-C, Graham DY. The eradication of *Helicobacter pylori* to prevent gastric cancer: a critical appraisal. *Expert Rev Gastroenterol Hepatol*. 2019;13(1):17–24.
- Xie YY, Yao LP, Yu XC, Ruan Y, Li Z, Guo JM. Action mechanisms and research methods of tRNA-derived small RNAs. *Signal Transduct Target Therapy*. 2020;5(1):1–9.
- Xu H, Wang C, Song H, Xu Y, Ji G. RNA-Seq profiling of circular RNAs in human colorectal cancer liver metastasis and the potential biomarkers. *Mol Cancer*. 2019;18(1):8.
- Xu W, Zhou B, Wang J, Tang L, Hu Q, Wang J, et al. tRNA-derived fragment tRF-Glu-TTC-027 regulates the progression of gastric carcinoma via MAPK signaling pathway. *Front Oncol*. 2021;11:733763.
- Yu MQ, Lu BJ, Zhang JS, Ding JW, Liu PY, Lu Y. tRNA-derived RNA fragments in cancer: current status and future perspectives. *J Hematol Oncol*. 2020;13(1):1–14.
- Yu X, Xie Y, Zhang S, Song X, Xiao B, Yan Z. tRNA-derived fragments: mechanisms underlying their regulation of gene expression and potential applications as therapeutic targets in cancers and virus infections. *Theranostics*. 2021;11(1):461–9.
- Zhang F, Shi J, Wu Z, Gao P, Zhang W, Qu B, et al. A 3'-tRNA-derived fragment enhances cell proliferation, migration and invasion in gastric cancer by targeting FBXO47. *Arch Biochem Biophys*. 2020;690:108467.
- Zhu L, Ge J, Li T, Shen Y, Guo J. tRNA-derived fragments and tRNA halves: the new players in cancers. *Cancer Lett*. 2019a;452:31–7.
- Zhu L, Li J, Gong Y, Wu Q, Tan S, Sun D, et al. Exosomal tRNA-derived small RNA as a promising biomarker for cancer diagnosis. *Mol Cancer*. 2019b;18(1):74.
- Zong TY, Yang YY, Zhao H, Li L, Liu MX, Fu XX, et al. tsRNAs: novel small molecules from cell function and regulatory mechanism to therapeutic targets. *Cell Prolif*. 2021;54(3):12977.

Publisher's Note

Springer Nature remains neutral with regard to jurisdictional claims in published maps and institutional affiliations.

Ready to submit your research? Choose BMC and benefit from:

- fast, convenient online submission
- thorough peer review by experienced researchers in your field
- rapid publication on acceptance
- support for research data, including large and complex data types
- gold Open Access which fosters wider collaboration and increased citations
- maximum visibility for your research: over 100M website views per year

At BMC, research is always in progress.

Learn more biomedcentral.com/submissions

